DEVELOPMENT OF PIV FOR MICROGRAVITY DIFFUSION FLAMES

Paul S. Greenberg[1], Mark P. Wernet[1], William Yanis[2],
David L. Urban[1], and Peter B. Sunderland[2]

[1]NASA Glenn Research Center
Cleveland Ohio

[2]National Center for Microgravity Research
Cleveland Ohio

INTRODUCTION

Despite numerous experimental investigations, the characterization of microgravity laminar jet diffusion flames remains incomplete. Measurements to date have included shapes, temperatures, soot properties, radiative emissions, and compositions, but full-field quantitative measurements of velocity have been limited. Kato et al. (1998) performed flame Particle Image Velocimetry (PIV) measurements in the JAMIC drop facility and Most et al. (2000) performed similar measurements on the AirBus A300 microgravity aircraft, but advanced PIV systems such as these have yet to be utilized in the NASA Glenn microgravity facilities. The present work concerns the development of a drop rig capable of performing PIV tests in diffusion flames in the 2.2 second drop tower.

Because the differences between normal-gravity and microgravity diffusion flames arise from changes in velocities, it is essential to measure velocity fields in microgravity flames. Velocity measurements in nonbuoyant flames will be helpful both in validating numerical models and in interpreting past microgravity combustion experiments. The importance of such measurements is mentioned in Law and Faeth (1994).

Pointwise velocity techniques, such as Laser Doppler Velocimetry, are inadequate for full-field velocity measurements in microgravity facilities. In contrast, the PIV system described here can capture an entire flowfield in 33 ms. Although PIV is a mature diagnostic for normal-gravity flames (Goss et al., 1991; Mungal et al., 1995; Driscoll and Mueller, 2002), restrictions on size, power and data storage complicate these measurements in microgravity.

Results are presented here from the application of PIV to the overfire region of a laminar gas jet diffusion flame in normal gravity. A methane flame burning in air at 0.98 bar was considered. The apparatus demonstrated here is packaged in a drop rig designed for use in the 2.2 second drop tower.

EXPERIMENTAL METHODS

The present flame was established in a windowed pressure vessel. The chamber internal width × depth × height were 25 × 25 × 50 cm. The tests were conducted in quiescent ambient air at 0.98 bar.

The burner was a 23 cm long stainless tube with an inside diameter of 5.5 mm. This length ensured fully developed laminar flow at the jet discharge. The burner was placed on the chamber centerline and oriented such that the methane injected vertically upward. The methane flowrate was maintained at approximately 1.1 mg/s. Fuel flowrate was controlled with a pressure regulator followed by a critical-flow metering valve. The chamber air was seeded prior to testing and the fuel was seeded during the tests.

The present PIV system is described in detail in Wernet et al. (2000). A dual-head mini-Nd:YAG laser operating at 532 nm was used to generate 50 mJ pulses. A 50×0.1 mm light sheet was generated using a 25 mm cylindrical lens and a 300 mm spherical lens.

The imaging system consisted of a 1008×1018 pixel Kodak ES 1.0 camera equipped with a 50 mm Schneider lens (set at f/2.8) and an interference filter (532 ± 10 nm). The first exposure had a 0.25 ms integration period. The second frame was integrated for 33 ms (while the first frame was being read from the sensor). Each pixel corresponded to a region of 51×51 μm in the object plane.

The PIV system hardware is based on custom designed in-house software, which provides the unattended operation required for the drop rig. All commercial PIV systems utilize graphical user interfaces, which are not amenable to automation. A Kodak ES 1.0 camera is coupled with an EPIX framgrabber board for "frame-straddling" image pair acquisition. The laser firing and camera timing are controlled via a National Instruments NI-6602 counter timer board. The NASA Glenn developed PIV system acquires image frame pairs at 15 Hz. The present velocity vector maps were obtained by averaging 100 instantaneous vector maps. Estimated velocity uncertainties are ±1% near the flame centerline and slightly higher in regions of lower velocity.

The data were multi-pass cross-correlation processed using 64×64 pixel subregions followed by 32×32 pixel subregions. The resulting velocity vector maps had horizontal and vertical spacings of 16 pixels, corresponding to grid point separations of 0.8 mm in the velocity vector maps. The analysis of the present PIV images used the correlation software of Wernet (1999).

The seed was 2.5 μm silica particles. These particles scatter sufficient light for these tests and are not expected to be significantly affected by thermophoresis. Microgravity rules out traditional seeders such as fluidized or packed beds, which can produce uncontrolled or overseeded conditions in microgravity. The present apparatus uses orifice-inlet seeders, which have been demonstrated in the microgravity facilities at NASA Glenn (Greenberg et al., 1997).

RESULTS AND DISCUSSION

A color image of the present flame is shown in Fig. 1. The flame was the longest nonflickering methane flame that could be obtained using the present burner in quiescent ambient air.

Figure 2 shows the velocity vectors and representative streamlines determined by PIV. The spatial resolution of the PIV measurements is the same as the spacing of the vectors in this figure. The streamline starting points are equally spaced at the upstream boundary. In this and subsequent figures, *HAB* is height above burner and the burner centerline corresponds to $r = 0$. Note that the present PIV measurements are in the overfire region but the present system also is capable of making velocity measurements within flames.

Figure 3 is a color contour plot of the velocity vectors of Fig. 2. Figure 4 is the corresponding contour plot of vorticity (assuming negligible gas velocities normal to the plane of the laser sheet). The present measurements took advantage of steady burning conditions by averaging over 100 PIV image pairs. Tests in the 2.2 second drop tower will not permit such extensive averaging. Nevertheless, Figs. 2-4 are representative of the velocity and vorticity measurements anticipated in upcoming microgravity combustion tests.

REFERENCES

Driscoll, J.F. and Mueller, C.J., Velocity Profiles Measured Across Wrinkled Flames – To Assess Flamelet Assumptions," *Combust. Sci. Technol.*, 179:9 (2002).

Goss, L.P., Post, M.E., Trump, D.D., and Sarka, B., "Two-Color Particle Image Velocimetry," *J. of Laser Applications*, winter, pp. 36-42 (1991).

Greenberg, P.S., Griffin, D.W., Weiland, K.J., and Yanis, W., "Selected Diagnostics for Microgravity Combustion Science;" Fourth International Workshop on Microgravity Combustion, Cleveland, pp. 275-280 (1997).

Kato, H., Kunieda, S., Enomoto, H., Okai, K., Kaneko, T., Chauveau, C., GöKalp, I., Sato, J., Tsue, M. and Kono, M., "Effects of Co-Flowing Air on Behavior of Gas Jet Diffusion Flames Under Normal- and Micro-gravity Fields," Drop Tower Days, JAMIC, paper 12-B-11, Sapporo, Japan (1998).

Law, C.K. and Faeth, G.M., "Opportunities and Challenges of Combustion in Microgravity," *Prog. Energy Combust. Sci.* 20:65 (1994).

Most, J.-M., Most, A., Susset, A., Baillargeat, J. and Joulain, P., "Flame Characterization by PIV in Microgravity Conditions," Tenth International Symposium on the Application of Laser Techniques in Fluid Mechanics, Lisbon (2000).

Mungal, M.G., Lourenco, L.M., and Krothapalli, A., "Instantaneous Velocity Measurements in Laminar and Turbulent Premixed Flames Using On-Line PIV," *Combust. Sci. Technol.*, 106:239 (1995).

Wernet, M.P., "Fuzzy Logic Enhanced Digital PIV Processing Software," 18th International Congress on Instrumentation for Aerospace Simulation Facilities, Toulouse, France (1999).

Wernet, M.P., Greenberg, P.S., Sunderland, P.B., and Yanis, W., "A PIV Investigation of Weakly Buoyant Laminar Get Diffusion Flames," AIAA-2000-0694, Reno (2000).
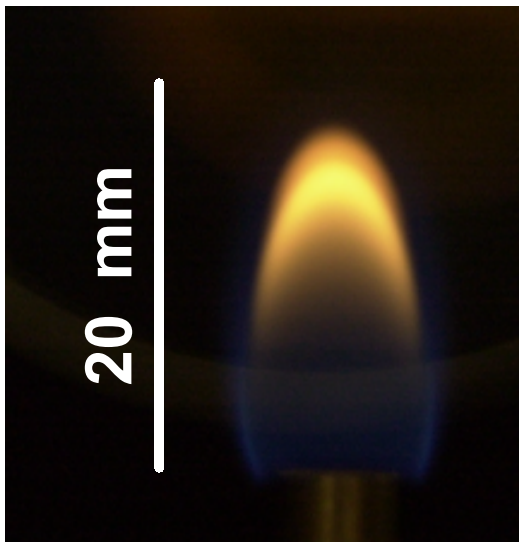
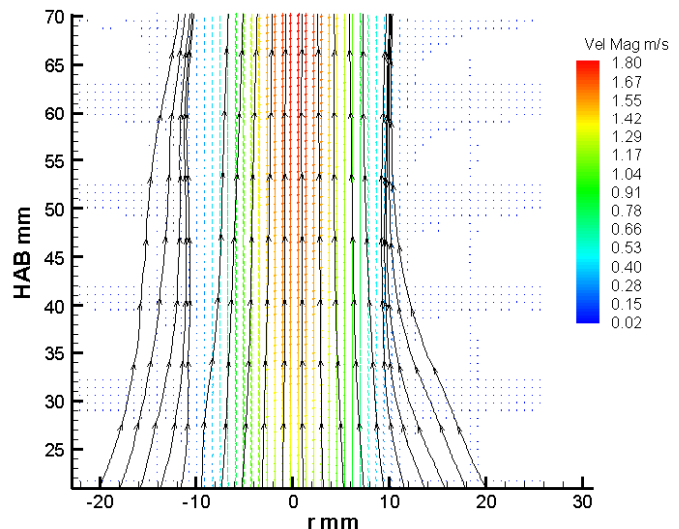Figure 1. Color image of the present flame and burner.

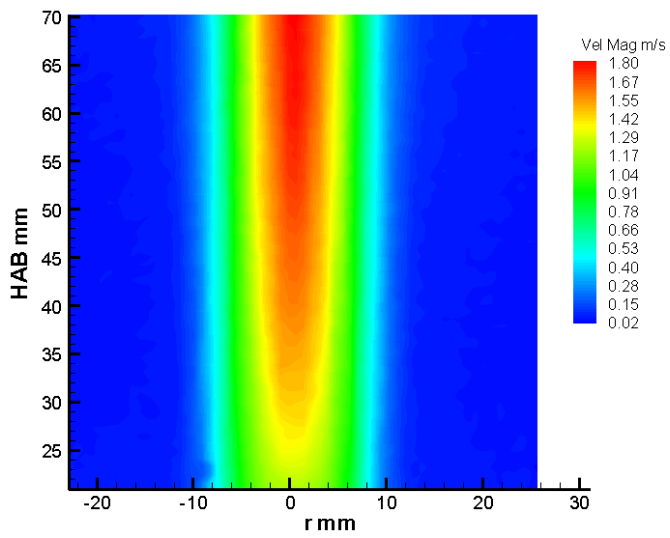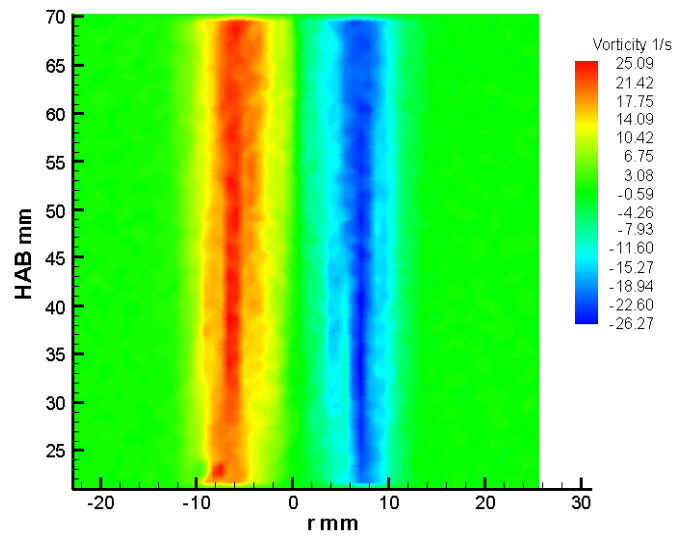Figure 2. Color velocity vectors and representative streamlines.

Figure 3. Color velocity contours.

Figure 4. Color vorticity contours.